USING THE TRIMBLE POST PROCESSED CENTERPOINT© RTX™ FAST POSITIONING SERVICE FOR HIGHLY ACCURATE UAS BASED MAPPING AND SURVEYING WITHOUT GNSS REFERENCE STATIONS

Omer Mian, Product Manager
Greg Lipa, Applications Specialist
Nilesh Gopaul, Navigation Analyst
Joe Hutton, Director
Srdjan Sobol, Product Manager
Applanix Corporation, 85 Leek Crescent,
Richmond Hill, ON, LB3 3B3
(OMian, GLipa, NGopaul, JHutton, SSobol)@applanix.com

ABSTRACT

Using Unmanned Aerial Systems (UAS) with an imaging sensor or LIDAR scanner to perform high accuracy mapping and surveying efficiently without the need for extensive Ground Control Points (GCPs) requires the computation of position and orientation to a very high degree of accuracy and precision. This is achieved using multi-frequency, multi-constellation Real-time Kinematic (RTK) and/or post-processed carrier phase Differential Global Navigation Satellite Systems (DGNSS) using a GNSS receiver on the UAS and a separate single GNSS reference station or network of stations located on the ground. To achieve centimetre-level accuracy, DGNSS techniques require that the distance between the single reference station (i.e., baseline) and the UAS trajectory be less than 20 km. Similarly, when a network of reference stations is employed, the distance should be less than around 70 km to the nearest station. For Visual Line of Sight (VLOS) UAS operations today, the GNSS baseline constraints are easily maintained. However, having to establish a suitable local reference station if a network is not available can add complexity and cost to operations. This cost and complexity will only grow as regulations change and UAS aircraft are allowed to operate Beyond Visual Line of Sight (BVLOS) from the observer. In this case, the need to set up local reference stations will severely limit productivity and increase data acquisition costs, especially in remote areas.

An alternative technique to DGNSS for high-accuracy positioning is known as Precise Point Positioning (PPP). Instead of differencing the rover observables from the reference station observables and cancelling out atmospheric and satellite errors, an advanced model for every aspect of the GNSS error chain is developed and parameterized. The Trimble Centerpoint RTX positioning solutions combine the methodology of PPP with advanced ambiguity resolution technology to produce centimetre-level positional accuracies without the need for local reference stations anywhere on the globe. The CenterPoint RTX is available with Standard and Fast convergence times, which is dependent upon the availability of regional atmospheric models. The time of convergence for the Standard service is better than 15 minutes, while the Fast service is less than 5 minutes.

This paper showcases the accuracy assessment of the Trimble Post-processed Centerpoint RTX Fast positioning technology (PP-RTX Fast) integrated into the Applanix POSPac UAV software for Direct Georeferencing of UAS mapping sensor data. A directly georeferenced mapping payload comprised of a Trimble APX-15 EI UAV with a Sony a7R camera used to produce highly accurate ortho-rectified imagery without ground control points was integrated into a DJI M600 platform.

The data logged by the APX-15 EI was processed in the Applanix POSPac UAV software using the PP-RTX Fast service to generate the Exterior Orientation (EO) for each image. The EO data was then entered into the Trimble's UASMaster photogrammetric software package along with the imagery to calibrate the camera during an airborne calibration flight, and to generate orthomosaics and Digital Surface Models (DSMs) for subsequent simulated production flights, without the use of GCPs. The accuracy of the calibration and the production flights were then quantified using independently surveyed checkpoints.

KEYWORDS: Unmanned Aerial Vehicle, UAV, Direct Georeferencing, Trimble Centerpoint RTX positioning, GNSS, Inertial, Mapping, Photogrammetry, Integrated Sensor Orientation, POSPac UAV, APX-15, Efficient Mapping

INTRODUCTION

Overview

The geospatial UAS community today is actively seeking new survey operation techniques and solutions that are automated, require minimal interaction with the user and above all are cost effective. Geospatial cloud processing platforms that merely require uploading the raw sensor data and output map products on demand without any interaction from the user are on the rise. On the data collection side, the UAS community is seeking for simplified logistics; no setting up of GNSS reference-stations or surveying of control points. Furthermore, for specific rapid response mapping applications, setting up a reference station may not be practical; this is where Applanix' Direct Georeferencing (DG) technology and Trimble's revolutionary Centerpoint RTX Fast positioning service excel.

This paper investigates how DG and Trimble Post-processed Centerpoint RTX Fast positioning technology allows the capture and generation of high accuracy survey grade map products from small Unmanned Aerial Systems (UAS) by:

- Eliminating the need to set up a GNSS reference station
- Eliminating GCPs
- Flying with minimal sidelap for improved field efficiencies and reduced costs

Direct Georeferencing

For aerial mapping applications, the EO of each image is required to produce map products such as orthomosaics and terrain models. Measurements from a differential GNSS system integrated with an Inertial Measurement Unit (IMU) such as the APX-15 (Figure 1) can be used for the direct determination of the EO parameters. This technique is known as Direct Georeferencing (DG).

Figure 1. Applanix APX-15 UAV Single Board GNSS-Aided Inertial solution for Direct Georeferencing on UAS

Post-processed CenterPoint RTX

The Trimble Post-processed CenterPoint RTX (PP-RTX) Standard service is a realization of the Trimble RTX technology implemented in the Applanix POSPac MMS and POSPac UAV software. It enables centimeter level trajectory generation from data logged by the Applanix GNSS-Inertial products without the need for local base stations. It is available globally via an internet connection [Hutton et al., 2016].

One of the prerequisites for using Standard PP-RTX for airborne mapping applications is trajectories of at least 30 - 40 minutes in duration with clean data (no cycle slips). This is to allow full convergence in the forward and reverse processing directions that is then removed in the combined solution with inertial data [Hutton et al., 2016]. The challenge with small UAS is that majority of these platforms are battery operated with very limited flight endurance (typically 15 to 30 minutes). With the introduction and rapid expansion of the Trimble's CenterPoint RTX Fast positioning service with a convergence time of fewer than 5 minutes, it is now feasible to reliably use PP-RTX corrections for high-accuracy UAV surveying and mapping. The PP-RTX Fast service is currently available in parts of the European Union and North America and is continuously being expanded on a worldwide basis. The accuracy specification for CenterPoint RTX is less than 4cm RMS horizontal, and 6cm RMS vertical.

PERFORMANCE TEST RESULTS

Test Overview

In July 2018, Applanix conducted a series of flights using a DJI M600 quadcopter, equipped with a Sony a7R camera (35mm AF-S Nikkor f/1.8 lens) and an APX-15 EI GNSS-Inertial system (Figure 2) installed on a Ronin active gimbal mount. The flights consisted of one calibration flight, and 3 simulated production flights over a test area.

Figure 2. DJI M600 UAS with the APX-15 EI UAV and a Sony a7R camera on Ronin Gimballed Mount

The APX-15 EI UAV is a GNSS-Inertial OEM solution designed to reduce the cost and improve the efficiency of mapping from UAS platforms. The APX-15 EI UAV contains a precision, survey grade GNSS receiver and dual inertial measurement units with identical performance; one embedded onto the GNSS-Inertial board located in the airframe and one as an external unit connected remotely to the imaging sensor. With this feature, the APX-15 EI can accurately and automatically translate the GNSS measurements from the GNSS antenna mounted on the airframe to the camera perspective centre on the gimbal mount without requiring an external interface. The Sony a7R is a prosumer digital RGB camera sensor, with a 36MP, 4.9-micron CCD producing images at 7360 columns by 4912 rows, configured with a 35 mm AF-S Nikkor f/1.8 lens. Both of these components were mounted to the M600 aircraft.

The Sony A7R was focused and then integrated with the APX-15 EI UAV on the Ronin MX mount. The mount is constructed in such a way as to maintain the stability of both the camera Interior Orientation (IO) and IMU boresight calibration over shock and vibration, thus turning the Sony a7R into a metric imaging solution. A Trimble SPS855 GNSS base station was set up in the project area to act as both as a reference solution and for surveying in the control point coordinates.

The timing of the Sony a7R sensor was previously characterized and calibrated to ensure that the imagery is accurately time-stamped at the mid-exposure pulse of the camera.

The test area consisted of a rectangular block, approximately 300m x 450m in size located north east of Toronto, Ontario, within the PP-RTX Fast coverage area. A network of approximately 15 control points comprised of photo identifiable metal targets was established within this test area (Figure 3) and surveyed using post processed DGNSS techniques with respect to the ITRF00 reference frame and UTM projection. The estimated accuracy of the control points coordinates is better than 2 cm RMS in each component (E, N, H). Some of these metal targets were attached to wooden structures (Figure 4), some were mounted on poles, and others were secured onto concrete slabs.

Figure 3. GCP distribution for the block viewed in Google Maps

Figure 4. Photo identifiable metal checkered target affixed to wooden structure

The calibration flight was flown over the block on July 19 and was conducted using two flying heights. The two flying heights allowed a more robust calibration of the camera focal length using 1 GCP. The principal points, lens distortion parameters and IMU-camera misalignment (boresight) angles were also obtained as part of the calibration. A total of 5 flight lines were flown at 100 m AGL (~1.5 cm Ground Sample Distance or GSD) in the North-East to South-West direction, and 3 perpendicular cross lines were flown at 60 m AGL (~1 cm GSD). Adjacent flight lines were always flown in opposite directions to ensure the best observability of the IMU boresight angles. The image side and end lap for the calibration flight were kept at 40% and 60% respectively.

On July 25, Applanix conducted a series of 3 simulated production flight tests over the same test site. In an ideal scenario, the calibration site and the site for the production flights should have been different locations, but this was not feasible due to logistical constraints. The goal of the flight campaign was to apply the camera IO and the IMU-camera misalignment (boresight) angles previously derived from the calibration flight to see if repeatable survey grade map products could be produced using only PP-RTX Fast and no base stations or GCPs. Each of the 3 missions was flown at 100 m AGL (~1.5 cm GSD) with 5 lines flown in the North-East to South-West direction (adjacent lines flown in opposite directions). The image side and end lap for each of these 3 flights were kept at 40% and 60% respectively.

For all missions, the relevant flight plans were created and uploaded into the UAS' flight management system. After take-off, the UAS proceeded to fly the survey lines autonomously.

The captured images and APX-15 EI UAV raw sensor data for each mission was subsequently downloaded from the payload sensor for processing and analysis.

Post Processing

The GNSS-Inertial data collected for all 4 flights (calibration and 3 production flights) using the APX-15 EI UAV system were post-processed in POSPac UAV software utilizing the PP-RTX Fast processing mode (Figure 5 and 6). The angles from the two inertial measurement units of the APX-15 EI UAV system were used to generate gimbal encoder angles to precisely produce the EO at the camera lens perspective centre, in the same datum, projection and epoch as the surveyed control points. The positional accuracy of the EO generated using the PP-RTX Fast processing mode for all flights was of the order of a few centimetres. Each EO along with its corresponding set of imagery was ingested into Trimble's UASMaster photogrammetric package for processing.

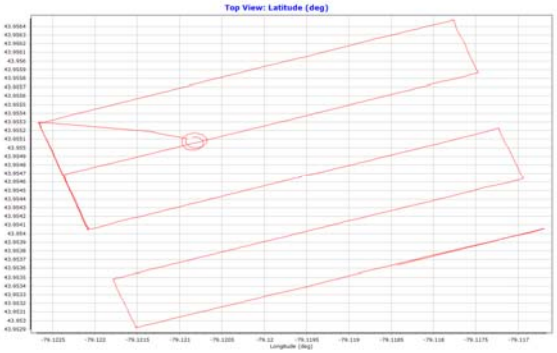

Figure 5. APX-15 UAV trajectory– Flight 1 on July 25

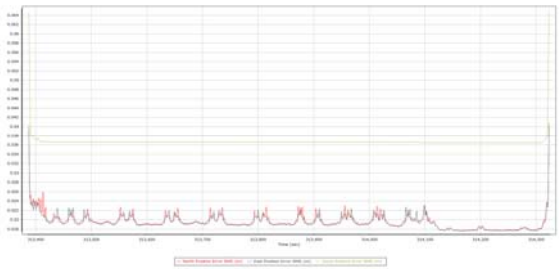

Figure 6. POSPac UAV trajectory RMS estimate – Flight 1 on July 25

Calibration Flight

For the calibration flight from July 19, approximately 33,000 tie points were extracted in UASMaster using the direct EO from POSPac UAV. The tie-points and direct EO were then run as part of a bundle adjustment. Using the two sets of flying heights, the IMU-camera misalignment (boresight) angles and full camera IO (i.e. focal length, principal point offsets and lens distortions parameters) were simultaneously estimated, by using only 1 GCP in the bundle adjustment.

The results of the camera and boresight calibration and the associated accuracy are summarised in Table 1 below:

Parameter	Value	RMS
Focal length [mm]	35.626	0.0261
Principal Point x [mm]	-0.129	0.0042
Principal Point y [mm]	-0.041	0.0042
K1	4.319E-05	N/A
K2	-1.575E-07	N/A
K3	2.474E-11	N/A
P1	-2.401E-05	N/A
P2	3.861E-05	N/A
Boresight Tx[deg]	-0.512	N/A
Boresight Ty[deg]	0.843	N/A
Boresight Tz[deg]	1.985	N/A

Table 1. Camera calibration accuracy

To check how well the calibration and the DG solution using PP-RTX fit the ground, the control points were used as checkpoints as part of the bundle adjustment. The checkpoint residuals for the calibration flight are summarized in the table below:

	Residuals (Errors)		
Point ID	dE	dN	dH
Check Point 1	-0.039	-0.004	-0.013
Check Point 2	-0.004	-0.030	-0.047
Check Point 3	-0.071	-0.035	-0.004
Check Point 4	-0.019	0.035	-0.002
Check Point 5	-0.048	0.016	0.017
Check Point 6	-0.049	0.055	-0.075
Check Point 7	0.002	-0.011	-0.038
Check Point 8	-0.001	-0.001	-0.061
Check Point 9	-0.004	-0.031	0.001
Check Point 10	0.000	-0.012	-0.013
Check Point 11	-0.038	0.005	-0.008
Check Point 12	-0.050	-0.032	0.062
Number of Points	**12**	**12**	**12**
Mean Error	**-0.027**	**-0.004**	**-0.015**
Standard Deviation (m)	**0.025**	**0.028**	**0.037**
RMSE (m)	**0.036**	**0.027**	**0.038**
RMSEr (m)	**0.045**	SQRT(RMSEx2 + RMSEy2)	
NSSDA Horizontal Accuracyr (ACCr) at 95%	**0.078**	RMSEr × 1.7308	
NSSDA Vertical Accuracyz (ACCz) at 95%	**0.075**	RMSEz × 1.9600	

Table 2. Calibration flight checkpoint residuals

Simulated Production Flights

The 3 flights from July 25 were also processed in UASMaster software (Figure 7) using the direct EO from POSPac UAV without GCPs. For these flights, the IMU-camera misalignment (boresight) angles and camera IO previously estimated from the airborne calibration flight on July 19 were entered and kept fixed, which meant the

bundle adjustment was only using the tie-points to refine the relative accuracy of the direct EO computed by POSPac UAV.

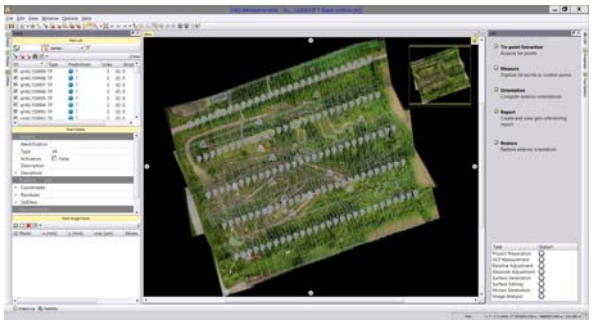

Figure 7. UASMaster Project

For each simulated production flight, a 1.5 cm GSD DSM was extracted and, in turn, used to orthorectify the images into a mosaic at a GSD of 1.5cm. A map view of the orthomosaic and DSM for Flight 1 are shown below (Figure 8 and 9).

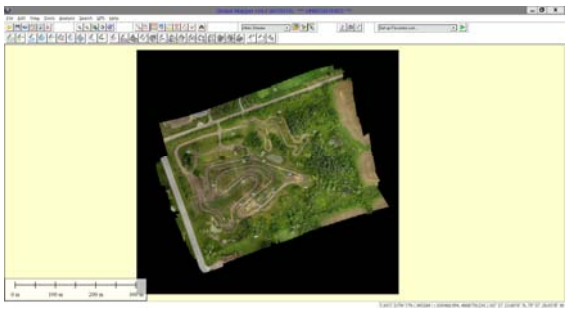

Figure 8. Control points overlaid on the orthomosiac displayed in Global Mapper software

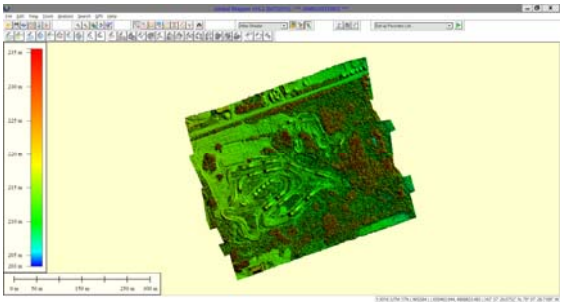

Figure 9. DSM displayed in Global Mapper software

The estimated map accuracy for each flight was then computed by measuring coordinates of the control points identified in the orthomosaics and DSM using Global Mapper. The results for each flight are summarized in the following Tables (Table 3, 4 and 5). A more detailed list of the results is presented in Appendix A.

Map Accuracy	dE	dN	dH
Number of Points	15	15	15
Mean Error	-0.011	-0.002	-0.087
Standard Deviation (m)	0.028	0.029	0.059
RMSE (m)	0.030	0.028	0.104
RMSEr (m)	0.041	SQRT(RMSEx2 + RMSEy2)	
NSSDA Horizontal Accuracyr (ACCr) at 95% Confidence Level	0.071	RMSEr × 1.7308	
NSSDA Vertical Accuracyz (ACCz) at 95% Confidence Level	0.204	RMSEz × 1.9600	

Table 3. Flight 1 Map Accuracy using PP-RTX and no GCPs

Map Accuracy	dE	dN	dH
Number of Points	15	15	15
Mean Error	-0.024	0.014	-0.090
Standard Deviation (m)	0.032	0.031	0.063
RMSE (m)	0.039	0.033	0.109
RMSEr (m)	0.051	SQRT(RMSEx2 + RMSEy2)	
NSSDA Horizontal Accuracyr (ACCr) at 95% Confidence Level	0.088	RMSEr × 1.7308	
NSSDA Vertical Accuracyz (ACCz) at 95% Confidence Level	0.213	RMSEz × 1.9600	

Table 4. Flight 2 Map Accuracy using PP-RTX and no GCPs

Map Accuracy	dE	dN	dH
Number of Points	15	15	15
Mean Error	-0.027	0.010	-0.085
Standard Deviation (m)	0.027	0.030	0.048
RMSE (m)	0.038	0.031	0.096
RMSEr (m)	0.049	SQRT(RMSEx2 + RMSEy2)	
NSSDA Horizontal Accuracyr (ACCr) at 95% Confidence Level	0.085	RMSEr × 1.7308	
NSSDA Vertical Accuracyz (ACCz) at 95% Confidence Level	0.189	RMSEz × 1.9600	

Table 5. Flight 3 Map Accuracy using PP-RTX and no GCPs

Observations and Discussion of Results

One of the challenges with airborne photogrammetry is the need to have an accurate camera calibration. This can be done terrestrially if the camera is stable at the pixel level over time (metric) or can be done in situ if the flight collections are designed in a way such that the calibration can be done as part of the Aerial Triangulation (AT) process (so-called self-calibration). The disadvantage of the former is the complexity of setting up a terrestrial calibration, while the disadvantage of the latter is the need for a well-designed block with lots of sidelap and endlap and GCPs to make sure the camera parameters and EO are mutually observable and correctly estimated, leading to inefficient data collection and excessive processing time.

The results of the calibration flight from July 19 and the 3 flights performed six days later using the same parameters show that the APX-15-EI Direct Georeferencing solution with post-processed RTX was accurate enough to calibrate the camera and IMU boresight from the air without the need for a base station or more than 40% sidelap only by using 1 GCP. It was also concluded that the lens distortions were accurately calibrated using this process, which means they can be held fixed and do not need to be re-estimated in subsequent processing since they rarely change over time (for higher end cameras and optics).

The results also show that the accuracy of the APX-15 EI UAV using PP-RTX Fast when integrated with a Sony a7R camera and a 35mm lens integrated into a Ronin gimbal mount and flown on an M600 platform has the potential to produce map products to an accuracy of ~4cm (3 pixels) horizontal RMS and ~10 cm (7 pixels) vertical RMS without a GNSS reference station or GCPs. These levels of absolute horizontal and vertical map accuracies are more than adequate for many surveying and mapping activities.

One observation is that the vertical results for all 3 flights flown on July 25 using PP-RTX Fast are biased by approximately 10 cm with standard deviations varying from 5 to 6 cm. This bias is probably due to a residual error in the focal length calibration that was being held fixed in the map production process. To verify this, Flight 1 was re-processed using the direct EO computed using the dedicated GNSS reference station instead of PP-RTX. In this case, a bias of around 7cm against the control points was still observed (Table 6), indicating that the vertical offset in the PP-RTX results is most likely related to a residual camera calibration error.

Map Accuracy	dE	dN	dH
Number of Points	15	15	15
Mean Error	0.002	-0.022	-0.013
Standard Deviation (m)	0.034	0.033	0.067
RMSE (m)	0.033	0.039	0.066
RMSEr (m)	0.051	SQRT(RMSEx2 + RMSEy2)	
NSSDA Horizontal Accuracyr (ACCr) at 95% Confidence Level	0.088	RMSEr × 1.7308	
NSSDA Vertical Accuracyz (ACCz) at 95% Confidence Level	0.130	RMSEz × 1.9600	

Table 6. Flight 1 Map Accuracy using a dedicated GNSS reference station and no GCPs

CONCLUSIONS

The test results illustrate the potential of using Post processed RTX Fast and Direct Georeferencing to:

- Provide sufficient accuracy to precisely calibrate the Interior Orientation of a camera and IMU boresight from the air by using only 1 GCP
- Generate map products to 4 cm RMS Horizontal and 10 cm RMS Vertical accuracy without the need to set up a base station or establish GCPs and use them in the photogrammetric process.

The results also show the outstanding capability of the APX-15-EI solution to automatically and accurately translate the GNSS positions from the antenna to the camera perspective centre when using a gimbal mount, and to fly with minimal side-lap to achieve maximum productivity.

FUTURE WORK

Future work will focus on attempting to improve the vertical performance of PP-RTX and evaluating its use with UAV based LIDAR.

REFERENCES

Hutton J. J., Gopaul N., Zhang X., Wang J., Menon V., Rieck D., Kipka A., Pastor F., 2016. Centimeter-level, robust GNSS-aided inertial post-processing for mobile mapping without local reference stations, ISPRS, Volume XLI-B3, 2016, pp. 819-826.

Mian O., Lutes J., Lipa G., Hutton J. J., Gavelle E., Borghini S., 2015. Direct georeferencing on small unmanned aerial platforms for improved reliability and accuracy of mapping without the need for ground control points, ISPRS, Volume XL-1/W4, 2015, pp.397-402.

Mostafa M.M.R, Hutton J., 2001. Direct Positioning and Orientation Systems, How Do they Work? What is the Attainable Accuracy? Proceedings ASPRS Annual Meeting, St. Louis, MO USA.

Hutton J., Mostafa M.M.R., 2005. 10 Years of Direct Georeferencing for Airborne Photogrammetry, Proceedings Photogrammetric Week, Stuttgart, Germany.

Ip A.W.L, El-Sheimy N., Hutton J., 2004. Performance Analysis of Integrated Sensor Orientation, International Archives of Photogrammetry and Remote Sensing, Istanbul, Turkey, ISPRS Comm. V, Vol. XXXV, Part B5, pp. 797-802.

APPENDIX A

	Survey Check Point Values			Map-derived values			Residuals (Errors)		
Point ID	E	N	H	E	N	H	dE	dN	dH
CheckPoint 1	650815.888	4868575.309	214.947	650815.917	4868575.319	215.056	-0.029	-0.010	-0.109
CheckPoint 2	650865.832	4868577.304	213.208	650865.836	4868577.288	213.289	-0.004	0.016	-0.081
CheckPoint 3	650929.352	4868543.972	213.279	650929.343	4868543.978	213.425	0.009	-0.006	-0.146
CheckPoint 4	650888.715	4868499.215	213.935	650888.713	4868499.245	214.068	0.002	-0.030	-0.133
CheckPoint 5	650855.198	4868465.242	214.695	650855.210	4868465.289	214.808	-0.012	-0.047	-0.113
CheckPoint 6	650839.419	4868494.264	213.482	650839.420	4868494.283	213.598	-0.001	-0.019	-0.116
CheckPoint 7	650806.859	4868469.191	214.862	650806.889	4868469.220	214.904	-0.030	-0.029	-0.042
CheckPoint 8	650740.613	4868515.962	215.231	650740.613	4868515.962	215.244	0.000	0.000	-0.013
CheckPoint 9	650814.550	4868526.715	213.917	650814.570	4868526.709	213.974	-0.020	0.006	-0.057
CheckPoint 10	650678.204	4868601.380	214.074	650678.204	4868601.380	214.103	0.000	0.000	-0.029
CheckPoint 11	650789.348	4868646.096	212.116	650789.367	4868646.100	212.189	-0.019	-0.004	-0.073
CheckPoint 12	650903.807	4868700.215	211.980	650903.888	4868700.137	211.973	-0.081	0.078	0.007
CheckPoint 13	650991.657	4868652.422	211.498	650991.618	4868652.391	211.720	0.039	0.031	-0.222
CheckPoint 14	650970.788	4868511.807	210.319	650970.767	4868511.811	210.438	0.021	-0.004	-0.119
CheckPoint 15	650767.221	4868379.890	213.726	650767.266	4868379.896	213.789	-0.045	-0.006	-0.063
Number of Points							**15**	**15**	**15**
Mean Error							**-0.011**	**-0.002**	**-0.087**
Standard Deviation (m)							**0.028**	**0.029**	**0.059**
RMSE (m)							**0.030**	**0.028**	**0.104**
RMSEr (m)							**0.041**	SQRT(RMSEx2 + RMSEy2)	
NSSDA Horizontal Accuracyr (ACCr) at 95% Confidence Level							**0.071**	RMSEr × 1.7308	
NSSDA Vertical Accuracyz (ACCz) at 95% Confidence Level							**0.204**	RMSEz × 1.9600	

Table A1. Map Accuracy- Flight 1

	Survey Check Point Values			Map-derived values			Residuals (Errors)		
Point ID	E	N	H	E	N	H	dE	dN	dH
CheckPoint 1	650815.888	4868575.309	214.947	650815.920	4868575.305	215.059	-0.032	0.004	-0.112
CheckPoint 2	650865.832	4868577.304	213.208	650865.832	4868577.304	213.320	0.000	0.000	-0.112
CheckPoint 3	650929.352	4868543.972	213.279	650929.364	4868543.954	213.399	-0.012	0.018	-0.120
CheckPoint 4	650888.715	4868499.215	213.935	650888.741	4868499.234	214.050	-0.026	-0.019	-0.115
CheckPoint 5	650855.198	4868465.242	214.695	650855.238	4868465.255	214.796	-0.040	-0.013	-0.101
CheckPoint 6	650839.419	4868494.264	213.482	650839.433	4868494.254	213.577	-0.014	0.010	-0.095
CheckPoint 7	650806.859	4868469.191	214.862	650806.899	4868469.185	214.899	-0.040	0.006	-0.037
CheckPoint 8	650740.613	4868515.962	215.231	650740.640	4868515.942	215.268	-0.027	0.020	-0.037
CheckPoint 9	650814.550	4868526.715	213.917	650814.601	4868526.686	213.982	-0.051	0.029	-0.065
CheckPoint 10	650678.204	4868601.380	214.074	650678.204	4868601.380	214.135	0.000	0.000	-0.061
CheckPoint 11	650789.348	4868646.096	212.116	650789.404	4868646.079	212.197	-0.056	0.017	-0.081
CheckPoint 12	650903.807	4868700.215	211.980	650903.886	4868700.122	212.007	-0.079	0.093	-0.027
CheckPoint 13	650991.657	4868652.422	211.498	650991.602	4868652.353	211.775	0.055	0.069	-0.277
CheckPoint 14	650970.788	4868511.807	210.319	650970.778	4868511.808	210.419	0.010	-0.001	-0.100
CheckPoint 15	650767.221	4868379.890	213.726	650767.266	4868379.905	213.738	-0.045	-0.015	-0.012
Number of Points							**15**	**15**	**15**
Mean Error							**-0.023**	**0.015**	**-0.089**
Standard Deviation (m)							**0.033**	**0.032**	**0.065**
RMSE (m)							**0.039**	**0.033**	**0.109**
RMSEr (m)							**0.051**	SQRT(RMSEx2 + RMSEy2)	
NSSDA Horizontal Accuracyr (ACCr) at 95% Confidence Level							**0.088**	RMSEr × 1.7308	
NSSDA Vertical Accuracyz (ACCz) at 95% Confidence Level							**0.213**	RMSEz × 1.9600	

Table A2. Map Accuracy- Flight 2

	Survey Check Point Values			Map-derived values			Residuals (Errors)		
Point ID	E	N	H	E	N	H	dE	dN	dH
CheckPoint 1	650815.888	4868575.309	214.947	650815.924	4868575.298	215.046	-0.036	0.011	-0.099
CheckPoint 2	650865.832	4868577.304	213.208	650865.846	4868577.286	213.300	-0.014	0.018	-0.092
CheckPoint 3	650929.352	4868543.972	213.279	650929.375	4868543.958	213.396	-0.023	0.014	-0.117
CheckPoint 4	650888.715	4868499.215	213.935	650888.740	4868499.235	214.042	-0.025	-0.020	-0.107
CheckPoint 5	650855.198	4868465.242	214.695	650855.232	4868465.258	214.796	-0.034	-0.016	-0.101
CheckPoint 6	650839.419	4868494.264	213.482	650839.419	4868494.264	213.572	0.000	0.000	-0.090
CheckPoint 7	650806.859	4868469.191	214.862	650806.892	4868469.203	214.918	-0.033	-0.012	-0.056
CheckPoint 8	650740.613	4868515.962	215.231	650740.645	4868515.950	215.261	-0.032	0.012	-0.030
CheckPoint 9	650814.550	4868526.715	213.917	650814.588	4868526.709	213.983	-0.038	0.006	-0.066
CheckPoint 10	650678.204	4868601.380	214.074	650678.235	4868601.361	214.147	-0.031	0.019	-0.073
CheckPoint 11	650789.348	4868646.096	212.116	650789.406	4868646.079	212.211	-0.058	0.017	-0.095
CheckPoint 12	650903.807	4868700.215	211.980	650903.876	4868700.113	211.991	-0.069	0.102	-0.011
CheckPoint 13	650991.657	4868652.422	211.498	650991.626	4868652.385	211.692	0.031	0.037	-0.194
CheckPoint 14	650970.788	4868511.807	210.319	650970.777	4868511.822	210.451	0.011	-0.015	-0.132
CheckPoint 15	650767.221	4868379.890	213.726	650767.283	4868379.906	213.733	-0.062	-0.016	-0.007
Number of Points							**15**	**15**	**15**
Mean Error							**-0.027**	**0.010**	**-0.085**
Standard Deviation (m)							**0.027**	**0.030**	**0.048**
RMSE (m)							**0.038**	**0.031**	**0.096**
RMSEr (m)							**0.049**	SQRT(RMSEx2 + RMSEy2)	
NSSDA Horizontal Accuracyr (ACCr) at 95% Confidence Level							**0.085**	RMSEr × 1.7308	
NSSDA Vertical Accuracyz (ACCz) at 95% Confidence Level							**0.189**	RMSEz × 1.9600	

Table A3. Map Accuracy- Flight 3